

# Spectral reflectance variability of skin and attributing factors

Catherine C. Cooksey, Benjamin K. Tsai, and David W. Allen  
Sensor Science Division  
National Institute of Standards and Technology  
Gaithersburg, MD, USA 20899

## ABSTRACT

Knowledge of the spectral reflectance signature of human skin over a wide spectral range will help advance the development of sensing systems for many applications, ranging from medical treatment to security technology. A critical component of the signature of human skin is the variability across the population. We describe a simple measurement method to measure human skin reflectance of the inside of the forearm. The variability of the reflectance spectra for a number of subjects measured at NIST is determined using statistical methods. The degree of variability is explored and discussed. We also propose a method for collaborating with other scientists, outside of NIST, to expand the data set of signatures to include a more diverse population and perform a meta-analysis to further investigate the variability of human skin reflectance.

Keywords: Skin, spectral, reflectance, traceable data, reference data, signatures, variability

## 1. INTRODUCTION

The optical properties of human skin have been of interest to researchers for some time. Their interest is based on a need to know for variety of different applications, which range from spectral imaging for automated or stand-off detection<sup>1-3</sup> to non-invasive clinical diagnostic tools<sup>4-7</sup> to improved models for understanding light propagation<sup>8</sup>.

The biological basis for the optical properties of human skin has been discussed in a number of review articles<sup>9-12</sup>. Human skin consists of multiple, non-homogeneous layers with numerous components, each having its own optical characteristics. In general, skin is composed of the epidermis and the dermis. The epidermis is nonvascular, consisting mostly of keratinocytes. Melanocytes are distributed throughout the deepest portions of the epidermis and produce the epidermis's main absorber, melanin. The dermis is vascularized, consisting mainly of collagen and elastin fibers. This layer's main absorbers are hemoglobin and water.

Although the reflectance spectra of human skin is the result of complex absorption and scattering events, it is typically described in terms of the absorption of melanin, oxy- and deoxygenated hemoglobin, and water<sup>11</sup>. Scattering also occurs. It has been estimated that 4% to 7% of light is reflected from the skin's surface across the solar reflective region<sup>9,12</sup>. Scattering by most of the skin's components is generally considered to be forward-directed<sup>9,11</sup>. Bashkatov, *et. al.* estimated the optical penetration depth of light into human skin over the spectral range of 400 nm to 2000 nm<sup>10</sup>. The penetration depth increases as wavelength increases, reaching a maximum of 3.5 mm near 1090 nm. Qualitatively, this suggests that ultraviolet radiation largely probes the epidermis, while visible to near-infrared radiation probes the dermal layer.

There have been numerous attempts to measure reflectance spectra of human skin, and the aims of these studies is varied. Researchers have investigated the optical properties (absorption coefficient, reduced scattering coefficient, and penetration depth) of *in vitro* skin samples using a spectrophotometer equipped with an integrating sphere, which enables measurement in both reflectance and transmittance modes<sup>10</sup>. Integrating sphere-based spectrophotometers or spectrometers have also been used to measure the reflectance of skin *in vivo*<sup>4,13</sup>. Researchers interested in the use of non-invasive, optical methods for clinical diagnostics have used fiber optic probes at the surface of the skin to detect the reflectance of skin *in vivo*<sup>5-7</sup>. The collection of reflectance measurements of skin *in vivo* using field spectroradiometers has also been demonstrated<sup>3</sup>. The spectral ranges investigated in these studies typically focused

on the visible range or the near infrared, where the signatures for hemoglobin and water, respectively, are most easily detected.

The aim of this study is to investigate the variability of the human skin reflectance spectra across a population and wide spectral range. We have previously reported that the overall variability of skin reflectance can primarily be attributed to biological variability among individuals<sup>14</sup>. In this paper, we report on the characteristics and variability of reflectance spectra collected for 51 subjects using a measurement method that directly ties measured reflectance spectra to the NIST scale of spectral reflectance and probes a broad spectral range, 250 nm to 2500 nm, in order to provide a foundational data set that can be utilized for a wide variety of applications. We also discuss briefly a proposal to collaborate with other scientists to expand this data set and gain a greater understanding of the variability of human skin reflectance.

## 2. MEASUREMENT METHOD

### 2.1. Image collection and reflectance measurement of human subjects

The method for collecting skin reflectance measurements of human subjects has been previously established and is described in detail in References 14 and 15. Briefly, it consisted of two parts, the collection of a photographic image of the subject's skin using a digital camera and the measurement of the reflectance of the subject's skin using a commercial spectrophotometer.

The test area was a 2.54 cm diameter circle located on the inside of the subject's right forearm. This test area was chosen for practical reasons, namely ease of measurement with the spectrophotometer and decreased prevalence of body hair and sun damage. The photograph was intended to document the visual appearance of the skin including non-uniformities, such as the presence of freckles, moles, or hair. The spectrophotometer was used to acquire the 8°/h spectral reflectance factor of the subject's skin within the test area over the spectral range of 250 nm to 2500 nm at a wavelength interval of 3 nm. For each subject, 3 scans were collected, each lasting approximately 3 minutes. The subject was allowed to rest their arm for approximately 3 minutes in between each scan.

The total number of subjects participating in this study\* was 51. All of the subjects were federal employees. There was no attempt to select subjects based on age, gender, or ethnicity as might be related to skin tone. No subjects were excluded for the use of sun screen, body lotion, or medication, or for the presence of freckles, moles, tattoos, or skin conditions or disorders.

### 2.2. Calculation of reflectance factors and associated uncertainties

The reflectance values obtained using the spectrophotometer were determined by a relative measurement. The reference standard used for these measurements was sintered polytetrafluoroethylene (PTFE). The spectral reflectance factors for sintered PTFE are traceable to the scale for spectral reflectance factor of pressed PTFE as established using the absolute method of Van den Akker<sup>16</sup> in the NIST Spectral Tri-function Automated Reference Reflectometer (STARR) facility<sup>17</sup>.

The 8°/h spectral reflectance factor  $R$  at each wavelength  $\lambda$  of the item was calculated from

$$R(\lambda) = \frac{S(\lambda) - S_d(\lambda)}{S_s(\lambda) - S_d(\lambda)} \cdot R_s(\lambda), \quad (1)$$

where  $S$  is the average signal from the scan of the item,  $S_s$  is the average signal from the scan of the standard,  $S_d$  is the dark signal, and  $R_s$  is the 8°/h spectral reflectance factor of the sintered PTFE standard. Dark signals were acquired

---

\* This human subject study, "Reflectance Measurements of Human Skin" Protocol #382, was initially approved by the NIST Institutional Review Board on May 29, 2012. Re-approval for continued collection of skin reflectance measurements was granted on September 19, 2013 and December 17, 2014.

once, prior to measurement session with a given subject. The final 8°/h spectral reflectance factors were obtained by averaging the values from the three scans.

The estimated measurement uncertainties for the reflectance measurements are calculated according to the procedures outlined in Reference 18 and are described in detail in References 14 and 15. Sources of uncertainty are the 8°/h spectral reflectance factor of the sintered PTFE standard, the sphere geometry, the wavelength, and random effects or repeatability. The evaluated contributions for these sources and the expanded uncertainty ( $k = 2$ ) are given in Table 1. These uncertainties represent the uncertainty associated with the spectrophotometer and measurement method used in this study. It is henceforth referred to as the instrument uncertainty.

**Table 1. Measurement uncertainties**

Source of Uncertainty	Standard Uncertainty	Uncertainty Contribution
Reflectance Standard	0.0045	0.0045
Geometry	0.001	0.001
Wavelength	0.3 nm	0.0008
Repeatability	0.0003	0.0003
		<b>Expanded Uncertainty (<math>k = 2</math>)</b>
		0.0094

### 3. NIST RESULTS AND ANALYSIS

#### 3.1. Images and reflectance spectra of human subjects

Consistent with our previous study<sup>14</sup>, inspection of the images revealed that each subject’s skin is generally uniform within the test area with only a minimal presence of veins and hair.

Selected reflectance spectra from the set of spectra collected from the 51 human subjects in this study are shown in Figure 1. The spectrum depicted by the black dashed curve is representative of the mean spectral reflectance values of all subjects participating in this study. The representative spectrum was selected from among the set of reflectance spectra based on its similarity to the mean spectrum using the following equation:

$$\theta_i = \cos^{-1} \left( \frac{S_m^T S_i}{\|S_m\| \|S_i\|} \right) \quad (2)$$

$S_m$  is the mean spectrum of reflectance factors for the full set of scans acquired (153 scans) and  $S_i$  is an individual spectrum from the set of scans. The difference between the spectra,  $\theta_i$ , is reported in radians. The spectrum with the smallest resulting angle is considered to be the closest match to the mean spectrum, and is selected as the representative of the mean. Selecting a representative spectrum from the overall set prevented the loss of spectral features that would have resulted from averaging the small shifts inherent in the spectral variability.

The variability observed for the set of subjects in this study was calculated using the standard deviation of the full set of scans. This variability, referred to as the population variability, is depicted in Figure 1 by the grey shaded area about the representative of the mean. The spectra (grey solid) representing the total range of observed reflectance factors in the ultraviolet (UV), visible (Vis), and near infrared (NIR) spectral regions are also provided in Figure 1.

Qualitatively, the spectra shown in Figure 1 are consistent with previous reflectance measurements<sup>9,13</sup>. For all subjects, various water absorption peaks (970 nm, 1450 nm, and 1900 nm to 1925 nm) are apparent in the NIR and shortwave infrared (SWIR). (Note: Absorption peaks result in “valleys” in a reflectance spectrum.) These signatures indicate that the incident light is probing the hydrated dermal layer. Greater variation in spectral signatures of human skin is seen in the UV and Vis. While the absorption signatures for hemoglobin are obvious in the spectra for the representative of the mean and the upper range of observed reflectance factors, these signatures are nearly absent in

spectra for the lower range of observed reflectance factors. In this spectral region, the ability to probe the various blood-borne pigments is tempered by absorption of the light by the melanin present in the epidermis. For subjects with significant concentrations of melanin, several key absorption signatures for hemoglobin (410 nm, 540 nm, and 575 nm) are absent. This is consistent with our previous study which demonstrated the lack of signatures for some subjects in plots of the first derivative of the reflectance spectra<sup>14</sup>.

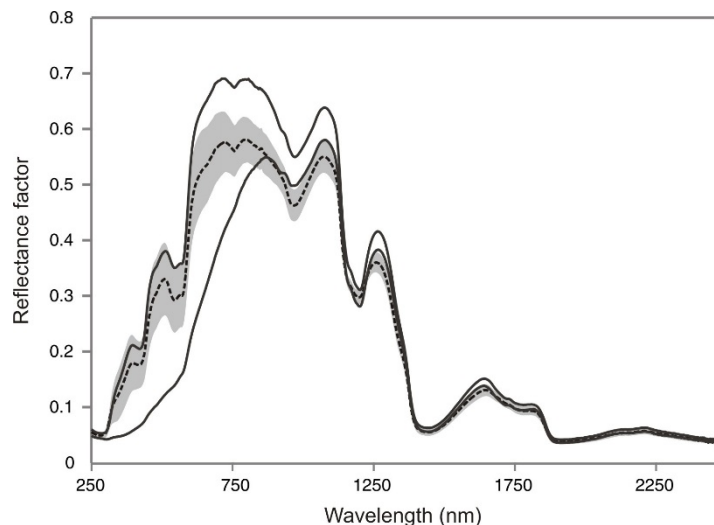


**Figure 1.** The reflectance spectrum of the representative of the mean (black dashed) with grey shaded area representing the population variability for all subjects. Representative spectra showing the range of variation in reflectance factors in the visible region (grey solid) are also depicted.

Figure 2 plots the population variability of this set of human subjects along with the instrument uncertainty (see Section 2.2) and the subject variability of representative subjects. The subject variability was calculated using the standard deviation of the three scans of several subjects. It represents the dynamic nature of human skin observed for each subject. Overall, the population variability is the most significant source of uncertainty for the skin's spectral signature over the UV-Vis-NIR region. In the SWIR, the instrument uncertainty is the dominant source of uncertainty.

### 3.2. Analysis

Quantification of the variability of the reflectance spectra for the 51 subjects can be accomplished by several methods. One method is spectral angle, which is a simple metric that quantifies the difference between spectra when treated as vectors<sup>19</sup>. It is sensitive to differences in spectral shape but insensitive to overall lightness or darkness. The spectral angle for all reflectance spectra was calculated according to Equation 2 for three arbitrary spectral regions (roughly corresponding to common detector responses) and the overall spectral range. The resulting spectral angles are listed in Table 2. The largest divergence occurs in the UV, followed by the VNIR and the SWIR, respectively. The full range is approximately equal to averaging the three individual ranges. These values closely match those reported in our previous study<sup>14</sup>, indicating that although the number of subjects has almost doubled, the population sampled here is similarly diverse.

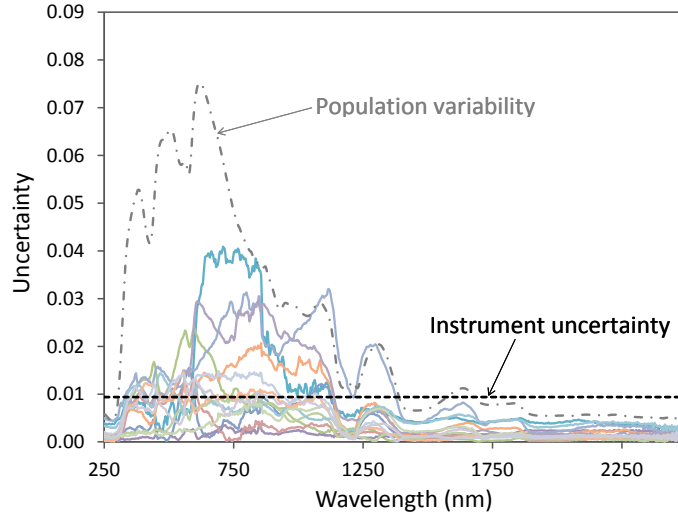


**Figure 2.** The instrument uncertainty (black dashed line), subject variability for several subjects (solid colored lines) and population variability for all subjects (grey dot-dashed line).

**Table 2.** The divergence of spectral angles, in radians, with respect to the mean spectrum of the full data set. The smaller the spectral angle the closer the match to the mean spectrum.

Wavelength Range (nm)	Spectral Angle (radians)			
	Minimum	Maximum	Mean	Standard Deviation
UV: 250 to 403	0.018	0.369	0.092	0.074
VNIR: 403 to 1003	0.006	0.267	0.046	0.050
SWIR: 1003 to 2500	0.007	0.112	0.030	0.015
Full: 250 to 2500	0.014	0.251	0.055	0.046

The spread of reflectance factors observed at several key wavelengths is shown in the histogram plots shown in Figure 3. The wavelengths chosen for this figure correspond to absorption peaks for hemoglobin (410 nm, 540 nm, and 575 nm) and water (970 nm and 1450 nm)<sup>5,10</sup>. The spread of reflectance factors observed is larger in the VNIR than that in the NIR and SWIR. The spread is particularly tight at 1450 nm, although it should be noted that overall uncertainty is comparable to the observed reflectance factors at this wavelength. The histograms are consistent with the results from the spectral angle analysis. Namely, the spread is largest for those wavelengths in spectral ranges that have the largest divergence from the mean.

The histograms also provide a measure of the diversity of the population sampled. For wavelengths 410 nm, 540 nm, and 575 nm where absorption by melanin competes with absorption by hemoglobin, the distribution is skewed towards higher reflectance factors. Whereas, at wavelengths 970 nm and 1450 nm where absorption of water dominates, the distribution is relatively symmetric.

Knowledge of the variability observed at these key wavelengths is crucial for applications which depend on these signatures to make diagnoses, such as the stand-off detection of cardiac pulse activities or determination of the level of skin hydration<sup>3,5</sup>.

In relation to human vision, the spectral features of each subject in the visible range can be described using the CIE color space coordinates, commonly referred to as CIELAB or CIE  $L^*a^*b^*$ <sup>20</sup>. These coordinates quantify visually discernable differences in color and lightness. The coordinate  $L^*$  represents the lightness of the color where  $L^* = 0$  indicates black and  $L^* = 100$  indicates diffuse white. The coordinates  $a^*$  and  $b^*$  represent color along the magenta-

green and yellow-blue continuums, respectively. The resulting CIELAB coordinates for all 51 subjects are plotted in Figure 4.

In the two-dimensional plot of the  $a^*$  and  $b^*$  coordinates, all subjects are clustered in the same region of the positive  $a^*b^*$  quadrant (magenta-yellow, respectively). Similar to the histogram plots in Figure 3, a skewed distribution of color coordinates is observed for this population. These results only provide a glimpse of the volume of color space that might be filled by a larger sample of the population. However, the results are consistent with previous attempts to describe the reflectance of human skin using CIELAB coordinates<sup>9</sup>.

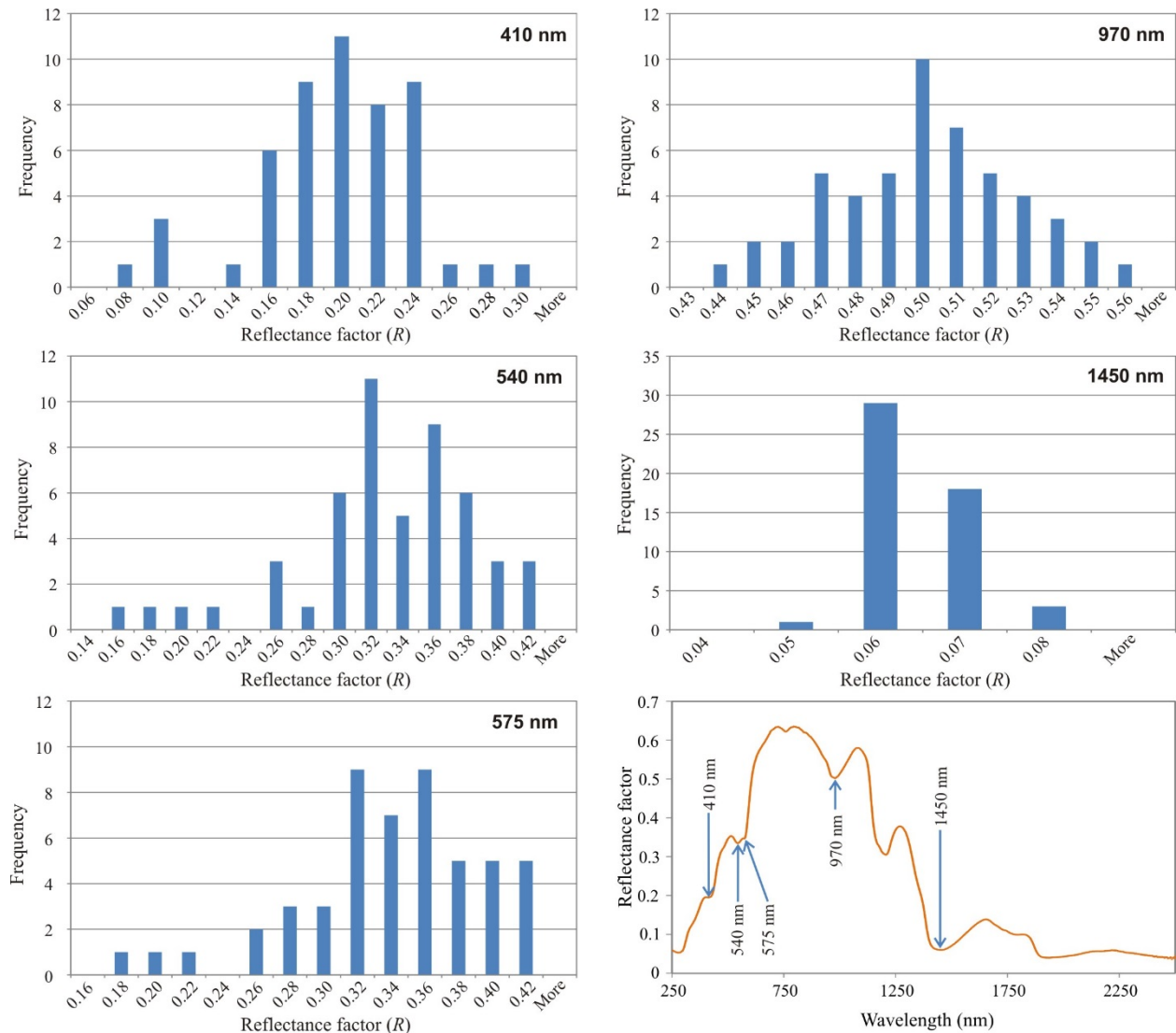


**Figure 3.** Histograms of the measured reflectance factors for all subjects at various wavelengths. The wavelengths are chosen to correspond to absorption peaks of skin components, hemoglobin (410 nm, 540 nm, and 575 nm) and water (970 nm and 1450 nm)<sup>5,10</sup>. A representative reflectance spectrum of human skin is shown at the bottom right with the wavelengths of these absorption peaks labeled.

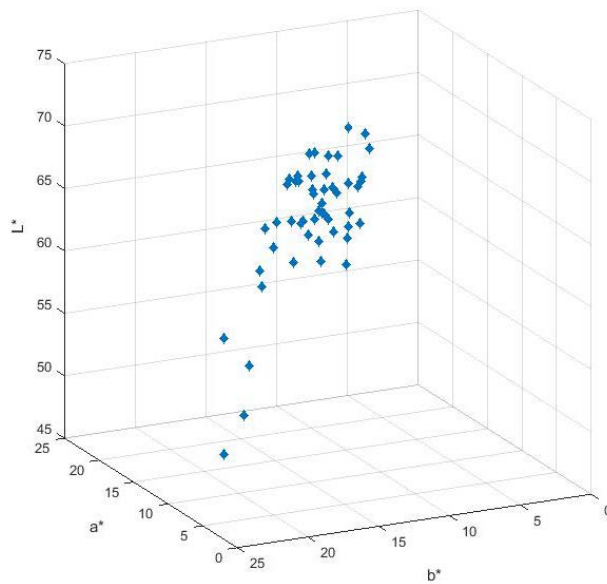


**Figure 4.** A three dimensional plot of the CIE L\*a\* b\* values for all subjects.

#### 4. COLLABORATION METHOD

It is not known what sample size or source of participants would best represent the population at-large. It can be expected that the variability is no smaller than the distribution presented here. Any one study will likely be limited and biased to local demographics. Thus, to address better the issue of inherent variability of skin reflectance, the authors will seek to expand this work to include studies performed elsewhere as a meta-analysis. Differences in a meta-analysis might be explained by the sources of variability discussed in the introduction and similarities might suggest that a sufficiently large sample size has been achieved.

#### ACKNOWLEDGEMENTS

The authors would like to thank the volunteers who took the time to contribute and were essential to this study.

\*\*Note: References are made to certain commercially available products in this paper to adequately specify the experimental procedures involved. Such identification does not imply recommendation or endorsement by the National Institute of Standards and Technology, nor does it imply that these products are the best for the purpose specified.

#### REFERENCES

- [1] Cooksey, C. C., Neira, J. E., and Allen, D.W., "The evaluation of hyperspectral imaging for the detection of person-borne threat objects over the 400nm to 1700 nm spectral region," Proc. SPIE 8357, 83570O (2012).
- [2] Angelopoulou, E., "Understanding the color of human skin," Proc SPIE 4299, 243-251 (2001).
- [3] Byrd, K.A., Kauer, B., and Hodgkin, V.A., "The use of spectral skin reflectivity and laser Doppler vibrometry data to determine the optimal site and wavelength to collect human vital sign signatures," ProcSPIE 8382, 83820F (2012).
- [4] Glennie, D.L., Hayward, J.E., McKee, D.E., and Farrell, T.J., "Inexpensive diffuse reflectance spectroscopy system for measuring changes in tissue optical properties," J. Biomed. Optics, 19(10), 105005 (2014).

- [5] Arimoto, H., Egawa, M., and Yamada, Y., "Depth profile of diffuse reflectance near-infrared spectroscopy for measurement of water content in skin," *Skin Res. Tech.* 11, 27-35 (2005).
- [6] Egawa, M., "In vivo simultaneous measurement of urea and water in the human stratum corneum by diffuse-reflectance near-infrared spectroscopy," *Skin Res. Tech.* 15, 195 (2008).
- [7] Kim, O., McMurdy, J., Lines, C., Duffy, S., Crawford, G., and Alber, M., "Reflectance spectrometry of normal and bruised human skins: experiments and modeling," *Physiol. Meas.* 33, 159-175 (2012).
- [8] Barun, V.V., and Ivanov, A.P., "Light scattering by a rough surface of human skin. 2. Diffuse reflectance," *Quantum Electronics*, 43(10), 979-987 (2013).
- [9] Anderson, R.R. and Parrish, J.A., "The optics of human skin," *J. Invest. Dermatol.* 77(1), 13-19 (1981).
- [10] Bashkatov, A.N., Genina, E.A., Kochubey, V.I., and Tuchin, V.V., "Optical properties of human skin, subcutaneous and mucous tissues in the wavelength range from 400 to 2000 nm," *J. Phys. D.* 38, 2543-2555 (2005).
- [11] Igarashi, T., Nishino, K., and Nayar, S.K., "The appearance of human skin," Technical Report: CUCS-024-05, Dept. of Computer Science, Columbia Univ. (2005); <http://www.cs.columbia.edu/techreports/cucs-024-05.pdf>, accessed 3/30/2014.
- [12] Lister, T., Wright, P.A., and Chappell, P.H., "Optical properties of human skin," *J. Biomed. Optics*, 17(9), 090901 (2012).
- [13] Dlugos, J.F., and Taylor, J.L., "Visible reflectance spectroscopy of human skin: The use of CIE L\*a\*b\* color analysis for in vivo ethnic skin characterization," Perkin Elmer Field Application Report (2012); [http://www.perkinelmer.com/CMSResources/Images/44-135750App\\_Visible-Reflectance-Spectroscopy-Human-Skin.pdf](http://www.perkinelmer.com/CMSResources/Images/44-135750App_Visible-Reflectance-Spectroscopy-Human-Skin.pdf), accessed 3/26/2014.
- [14] Cooksey, C. C., Tsai, B. K., and Allen, D. W., "A collection and statistical analysis of skin reflectance signatures for inherent variability over the 250 nm to 2500 nm spectral range," *Proc. SPIE* 9082, 908206 (2014).
- [15] Cooksey, C. C. and Allen, D. W., "Reflectance measurements of human skin from the ultraviolet to the shortwave infrared (250 nm to 2500 nm)," *Proc. SPIE* 8734, 87340N (2013).
- [16] Venable, W. H., Hsia, J. J., and Weidner, V. R., "Establishing a Scale of Directional-Hemispherical Reflectance Factor I: The Van den Akker Method," *J. Research of the Natl Bureau of Stnds*, 82(1), 29-55 (1977).
- [17] Barnes, P. Y., Early, E. A., and Parr, A. C., "NIST Measurement Services: Spectral Reflectance," NIST Special Publication 250-48 (1998).
- [18] Taylor, B. N. and Kuyatt, C. E., "Guidelines for Evaluating and Expressing the Uncertainty of NIST Measurement Results," NIST Technical Note 1297 (1994).
- [19] Kruse, F. A., Lefkoff, A. B., Boardman, J. B., Heidebrecht, K. B., Shapiro, A. T., Barloon, P. J., and Goetz, A. F. H., "The Spectral Image Processing System (SIPS) - Interactive Visualization and Analysis of Imaging spectrometer Data," *Remote Sensing of the Environment*, 44(2), 145-163 (1993).
- [20] ASTM E308-13, "Standard Practice for Computing the Colors of Objects by Using the CIE System."